




Multiple Seismic Reflection Attenuation Using High-Resolution Radon Filter Method: A Case Study for 2D Land Seismic Data, South of Iraq

Ahmed J. R. Al-Heety ^{1*} , Hassan Z. Ali ²

^{1,2} Department of Seismic processing /Oil Exploration Company (OEC), Ministry of oil Baghdad, Iraq.

Article information

Received: 03- Apr -2024

Revised: 03- June -2024

Accepted: 01- Jul -2024

Available online: 01- Jul – 2025

Keywords:

Seismic data
Multiple reflections
 τ -p domain
Radon filter
Multiple attenuations.

Correspondence:

Name: Ahmed J. R. Al-Heety

Email:

ahmedalheety@gmail.com

ABSTRACT

This article presents the pre-stack attenuation of multiple noises from a 2-D land seismic survey acquired on the Iraq-Kuwait border in southern Iraq. The processing workflow is performed using the Geovation software from CGG that employs a de-aliased High-Resolution Radon with a non-iterative process for seismic reflection data. First, we apply noise attenuation, surface deconvolution (predictive), and normal move-out (NMO) correction, which is executed using the root-mean-square velocity (RMS velocity) to flatten the primary event, and the Common Mid-Point gathers (CMP gathers) are converted into the Radon domain using a least-squares-parabolic Radon transform. Several tests are performed on some parameters to predict the multiple events using a High-Resolution de-aliased multiple attenuation (RAMUR) algorithm aimed to attenuate multiple events. RAMUR algorithms compute a model of primary and multiple events based on data decomposition into user-defined parabolas and are performed using a high-resolution, de-aliased least-squares method. The Radon transforms separate primary reflection and multiple reflection events in the (τ -q) domain based on move-out differences between primary and multiple events, which are characterized as events with slower velocity. Reflection events relating to parabolas with a higher curvature are counted as multiples, whereas events with smaller are counted as primary events. The RAMUR algorithms subtract the model of multiples from the input gathers. The workflow effectively attenuates reflection-based generated multiples events, which improves the overall seismic response after imaging, and enhances correlation with well information.

DOI: [10.33899/earth.2024.148493.1261](https://doi.org/10.33899/earth.2024.148493.1261), ©Authors, 2025, College of Science, University of Mosul.

This is an open access article under the CC BY 4.0 license (<http://creativecommons.org/licenses/by/4.0/>).

توهين الانعكاسات الزلزالية المتكررة باستخدام طريقة مرشح الرادون عالي الدقة: دراسة حالة لبيانات زلزالية انعكاسية ارضية ثنائية الأبعاد في جنوب العراق

أحمد جدوع الهيتي^{1*} , حسان زيد علي²

^{1,2} قسم معالجة البيانات الزلزالية، شركة الاستكشافات النفطية، وزارة النفط، بغداد، العراق.

ملخص	معلومات الارشفة
يعرض هذه البحث دراسة حالة لتوهين التكرارات (الضوضاء المنتظمة) لبيانات ما قبل النضد لتسجيلات المسح الزلزالي ثنائي الأبعاد التي تم تنفيذها على الحدود العراقية-الكويتية في جنوب العراق. تم تنفيذ سير عمل معالجة البيانات باستخدام برنامج CGG Geovation والذي يستخدم تحويلات الرادون عالي الدقة لبيانات الانعكاس الزلزالي. حيث تم أولاً توهين الضوضاء، وتطبيق عملية النقل (التبني)، والتصحيح الحركي الاعتيادي (NMO) والذي تم تنفيذه باستخدام معدل الجذر التربيعي (سرعة RMS) لتسوية الحدث الأساسي، وتحويل نقاط الوسط المشتركة (تجميع CMP) إلى مجال الرادون باستخدام تحويل الرادون ذي المربعات المكافئة الصغرى. تم إجراء العديد من الاختبارات على بعض المعلمات للتنبؤ بالأحداث الزلزالية المتكررة باستخدام خوارزمية توهين التكرارات RAMUR عالية الدقة، والتي كان هدفها توهين هذه التكرارات. تحسب خوارزميات RAMUR نموذجاً للأحداث الأولية والمتكررة بناءً على تحليل البيانات إلى قطع مكافئة محددة من قبل المستخدم ويتم تنفيذها باستخدام طريقة المربعات الصغرى عالية الدقة. يحول الرادون أحداث الانعكاس الأولي والمتكرر بشكل منفصل في مجال (τ-q) استناداً إلى الفروقات في السرعة ما بين الأحداث الأولية والمتكررة التي تتميز بأنها أحداث ذات سرعة أبطأ. يتم اعتبار أحداث الانعكاس المتعلقة بالقطع المكافئ ذات الانحناء الأعلى كمضاعفات، في حين يتم حساب الأحداث ذات القطع الأصغر كأحداث أولية. ومن ثم تقوم خوارزميات RAMUR بطرح نموذج التكرارات من المدخلات. تعمل خطوات سير العمل بشكل فعال على توهين الأحداث المتكررة الناتجة عن انعكاس الموجات، وتحسين الاستجابة الزلزالية الشاملة بعد التصوير، وتعزيز النتائج بربطها مع معلومات الآبار.	تاريخ الاستلام: 03-ابريل-2024 تاريخ المراجعة: 03-يونيو-2024 تاريخ القبول: 01-يوليو-2024 تاريخ النشر الإلكتروني: 01-يوليو-2025 الكلمات المفتاحية: البيانات الزلزالية الانعكاسات المتكررة مجال τ-p مرشح الرادون توهين التكرارات. المراسلة: الاسم: أحمد جدوع الهيتي Email: ahmedalheety@gmail.com

DOI: [10.3389/earth.2024.148493.1261](https://doi.org/10.3389/earth.2024.148493.1261), ©Authors, 2025, College of Science, University of Mosul.
This is an open access article under the CC BY 4.0 license (<http://creativecommons.org/licenses/by/4.0/>).

Introduction

The 2D seismic survey is carried out in southern Iraq near the Iraq-Kuwait border within the Gotnia Basin (Marlow *et al.*, 2014) above the Umm Qasr geological structure (UQ-1), which was drilled between 1978 and 1979. The Umm Qasr structure is an N-S trending anticline, whose tests revealed oil-bearing Mishrif, Nahr Umr, and Zubair formations (Jassim and Goff, 2006). However, since that time, no additional wells have been drilled. The drilling stopped due to technical problems within the Zubair Formation. It may show oil/gas from deep reservoirs such as Paleozoic, Jurassic, to Cretaceous formations (e.g., Mishrif, Nahr Umr, Zubair, Najma, and Chia Zairi). The perfect interpretation of seismic sections is one of the main important phases of oil/gas exploration and production. Hence, to reach this aim, the seismic images must be of good quality, and picked horizons correspond to the primary events, which are reflected from only a single subsurface interface. Any other event's form of energy is undesirable, for instance: surface noise, guided waves, ground roll, refractions, and multiple reflections.

Multiple attenuation has always been challenging in the field of seismic data processing. An important task in seismic data processing is identifying and suppressing multiple reflection events.

The multiple events were documented in the late 1940s, and the Geophysics issue (1948) was dedicated to papers discussing the multiple events and procedures for their recognition (Taner, 1980; Weglein, 1999). The multiple-reflection events are called coherent noise (Al-Heety and Thabit, 2022; Alvarez, 1995, 2001; Yilmaz, 2001) for most interpreters reflected at more than one interface or in other words from more than one impedance interface (horizon), and are known to hinder the primary reflections from the seismic data leading to ambiguity seismic interpretation, reservoir characterization, and seismic inversion, since they can be categorically false as primary events. Also, the events not only affect the seismic image, producing the structural and stratigraphical interpretations unreliable, but also affect the pre-stack data, reaching reliable Amplitude Variation with Offset or Angle/Azimuthal (AVO/AVA) and AVO attributes at the impure boundaries very problematic, if not impossible (Iverson *et al.*, 2014; Lacombe *et al.*, 2019; Yousif *et al.*, 2022; Gardi *et al.*, 2024). Furthermore, the achievement of the AVO results relies considerably upon the processing sequence employed, especially in the presence of intense multiple events and reverberations (Al Mukhtar and Alsayadi, 2015; Ramos *et al.*, 1999). The multiple reflection events offer one of the most significant problems in seismic exploration. Many following papers have discussed the subject of recognition and suppression of multiples. The first property of primary reflections is that they have less NMO than multiple events (Riley and Claerbout, 1976; Trinks, 2000; Y. Wang, 2004; Yilmaz and Doherty, 1987). Also, the primaries have less curvature than multiples (have longer arrival times than primaries). The other property of multiples that forms the basis of suppression is periodicity (Xiao *et al.*, 2003). The multiples usually lack the familiar periodicity accompanying marine multiples (Alvarez, 2001); in contrast, they are particularly not easy to distinguish from primary events in land data. Since they generally lack periodicity coupled with marine data multiples (Dix, 1948; Gutenberg and Fu, 1948; Waterman, 1948; Hansen and Johnson, 1948). Figure 1 shows some different modes of common forms of multiple reflections. Fig. 2 shows a common shot gathers and a corresponding sketch showing the main seismic events.

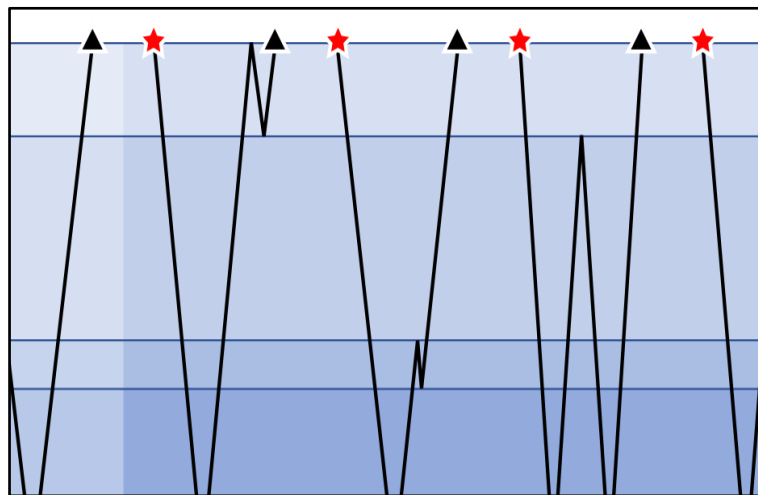


Fig. 1. A sketch showing different modes of multiple reflections.

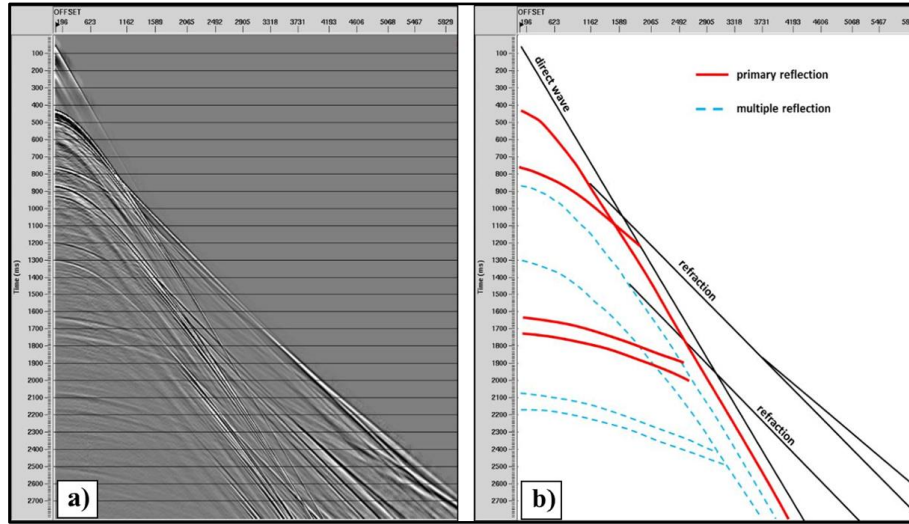


Fig. 2. (a) A common shot gathers and (b) a corresponding sketch showing the main seismic events (Kakhkhorov, 2019)

Based on their time delay (or based on their paths), the multiples are distinguished as short-path (period), indicating that they hinder the primary events. It is generated close to the primary so that it interferes with primary reflections from the same reflectors (Dix, 1948; Yilmaz and Doherty, 1987; Verschuur *et al.*, 1992; Weglein *et al.*, 1997; Geldart and Sheriff, 2004; Moore and Dragoset, 2008). It appears as a separate reflection on the seismic record, which might interfere with primary events at the same time (Al-Shuhail and Al-Dossary, 2020). The short-path multiples are more common in land data (e.g., ghosts, near-surface multiples, and peg-leg multiples). The long-period (path) multiples travelled more in the shallower (slower) part of the seismic section than primaries with a similar arrival time; therefore, they ordinarily show more NMO and can be attenuated by Common Mid-Point (CMP) stacking (Sheriff and Geldart, 1995). Typically, the long-path multiple events are very common in marine data. However, the long-path multiples are very common in marine data. Based on the downward reflection interface, multiple events are categorized into surface-related multiples (SRM) and internal multiples (IM). Overall, multiple attenuation methods (MAM) are classified into two major categories (Weglein, 1995, 1999):

1. Exploit the difference of a specific property between multiple and primary events. e.g., (predictive deconvolution, conventional f - k , and Radon, and statistical) methods.
2. Predict multiple energy and then subtract from seismic data (Dragoset and Jeričević, 1998).

Other authors classified MAM into three classes (Wang *et al.*, 2023): filtering-based methods (Treitel, 1969; Taner, 1980; Weglein *et al.*, 1997), Transformation methods in a particular domain (Foster and Mosher, 1992; Yilmaz, 2001; Schonewille and Aaron, 2007). The last class is the machine learning (ML) techniques (Tao *et al.*, 2022) and deep neural networks (Li *et al.*, 2021; Li and Gao, 2020; Wang *et al.*, 2022). Depending on the NMO-Velocities (V_{NMO}) differences, the multiples and primaries can be transformed into specific domains where they can be separated more effectively than the time domain (t - x domain). The common methods that use different V_{NMO} are f - k filtering (Sengbush, 1983), cluster filtering, and Radon transform-based methods (Hampson, 1986; Foster and Mosher, 1992; Sacchi and Ulrych, 1995; Hargreaves and Cooper, 2001; Li and Lu, 2014; Li and Yue, 2017; Trad, 2003).

Between the aforementioned MAM, the Radon transform-based techniques are commonly used in seismic data processing (Sacchi and Ulrych, 1995; Trad, 2003; Wang, 2004; Nowak and Imhof, 2006; Mahdad *et al.*, 2011; Ibrahim *et al.*, 2015; Xue *et al.*, 2016). In the Radon domain, the curvatures (q) of primaries are adjacent to zeros (after NMO), whereas they are larger than zeros for multiple events due to under-correction. The Radon transform methods can be divided into three categories according to the integral path: Hyperbolic, Parabolic, and Linear. However, the Parabolic Radon transform (PRT) is the most popular one used in multiple attenuations due to its efficiency in most situations (Hampson, 1986; Song *et al.*, 2022).

More recently, researchers (Sacchi and Ulrych, 1995; Hugonnet and Canadas, 1997; Cary, 1998; Sacchi and Porsani, 1999) have developed a High-Resolution Radon transform. Herrmann et al (2000) presented non-iterative de-Aliased High-Resolution (DHR) Radon spectra. This technique focuses on the parabolic *decomposition* of the data on the weightiest spectral components. This approach's basic assumption is that the signal is non-dispersive, meaning that the frequency components have roughly the same parabolic decomposition. The Parabolic Radon-filtering methods rely on velocity discrimination between the primary and multiple events. The CMP gathers after NMO will be modeled as a superposition of constant amplitude parabolas. The most curved parabolas, supposed to be the multiples (slower than the primaries), are retained and eliminated (subtracted) from the seismic data (Hugonnet *et al.*, 2009).

Aim of study

This current case study aims to test the used de-aliased High-Resolution (DHR) Parabolic Radon Transform (Tau-q domain) (RAMUR) algorithm on the 2D seismic data acquired in Iraq without any prior information to separate the multiple events from the primary events in seismic data, and to produce seismic data without multiples as a result for getting a better image of subsurface without interference with multiple events that make data misinterpreted.

Location and Geological Setting

The study area is located in the southern Mesopotamian basin, southern Iraq. Nearly all of the oil fields are located within the Mesopotamian foredeep, the Gotnia Basin, and the Zagros fold belt. More than 90 percent of the oil and gas occurs in reservoirs of the Cenozoic and Cretaceous ages. The part of largest reserves occurs in carbonate rocks (Mishrif Formation) and siliciclastic rocks (Zubair Formation) in fields within the Mesopotamian foredeep zone in southern Iraq, according to Iraq's tectonic division (Fouad, 2012), including (Rumaila, West Qurna, and Zubair) fields. Smaller reserves occur in Jurassic and Triassic carbonates, and Ordovician siliciclastic. The case study area lies in the Mesopotamian Zone within the Zubair Subzone, where the structures of this Subzone in southern Iraq are controlled by the basement structures (Faults) and infra-Cambrian brain salt (Jassim and Goff, 2006), and Alpine Orogenic Movements (Al-Sakini, 1995). The Mesopotamian Zone has a very thick sedimentary column ranging from Pleistocene to Jurassic succession (Jassim and Goff, 2006; Owen and Nasr, 1958). Figure 3 shows the general stratigraphic column of South Iraq, Basrah region.

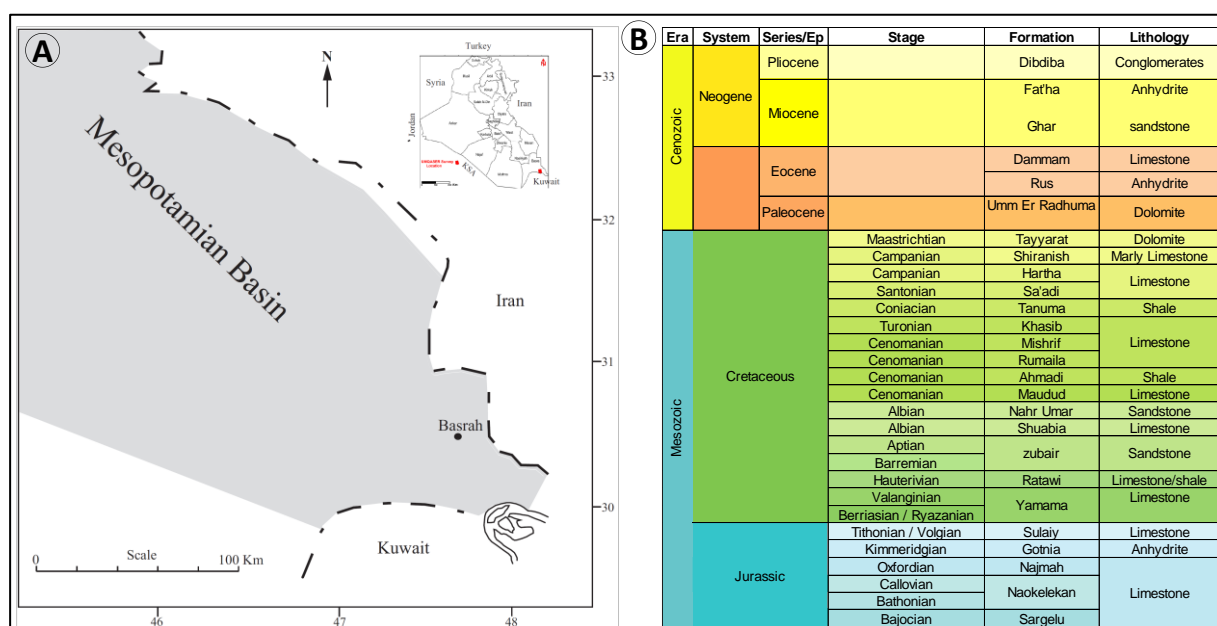


Fig. 3. (a) Location map of the study area showing Basrah region; (b) Stratigraphic column of South Iraq, Basrah region (modified from Al-Ameri *et al.*, 2012).

Materials and Methods

Seismic data in the Southern area of Iraq is strongly contaminated with multiple energies that impair the image of reservoir reflectors, impact the accuracy of structural and stratigraphic mapping, and the reliability of reservoir characterization within known reservoir formations, as well as the quantitative interpretation of the reservoir. The high impedance contrasts between carbonates and anhydrite geological layers with clastic are the major generators of the surface and interbed multiples in the south of Iraq. Based on testing and comparison with the Vertical Seismic Profiles (VSP) data from several wells in southern Iraq, it is concluded that the Cretaceous Tanuma and Ahmadi formations are the main multiple generators that contaminated the reservoir sequence. Unfortunately, in the current case study, the available well data within the survey area has no VSP measurement that helped us to determine the multiple generators. The Radon transform (RT) transforms data from the $(t-x)$ domain into the $(\tau-q)$ domain.

The Parabolic Radon ($\tau-q$) transform is one of the most used multiple attenuation methods to improve the separation of coherent events in the (CMP domain) to remove long-period multiples (Hampson, 1986; Yilmaz, 2001). The $(\tau-q)$ transform moves parabolic events after NMO to different areas of the parabolic Radon depending on the curvature of the events. The multiple events tend to follow a parabolic moveout after the NMO correction. The important steps in the Radon demultiple, as shown in Figure 4A, are: the data are first sorted in the CMP gathers domain; second, NMO correction is applied to the data so that primaries can be flattened while the curvatures of multiples become parabolic. The velocities must be picked with sufficient accuracy to distinguish primary energy from slightly slower multiple energies. The third step consists of transforming the data in the $(\tau-q)$ domain using the PRT. An event with a parabolic moveout in the time-offset domain is mapped to a point by using the RT. The multiples are then filtered, and a Radon inverse transform is performed to recover data without multiples.

Sacchi and Ulrych (1995) and Cary (1998) have a technologically advanced High-Resolution Radon transform (frequency or time domain). These constrain the radon spectra to be sparse in curvature (q) and intercept (t). Herrmann et al. (2000) presented de-aliased High-Resolution (DHR) Radon spectra with a non-iterative process. This non-iterative process without a priori information on the curvature of the multiples focuses the parabolic decomposition of the data onto its most weighty spectral components. The application of this approach leads to remarkable results. Figure 4B shows the power of the DHR Radon algorithm to separate multiples from primaries with a large move-out divergence.

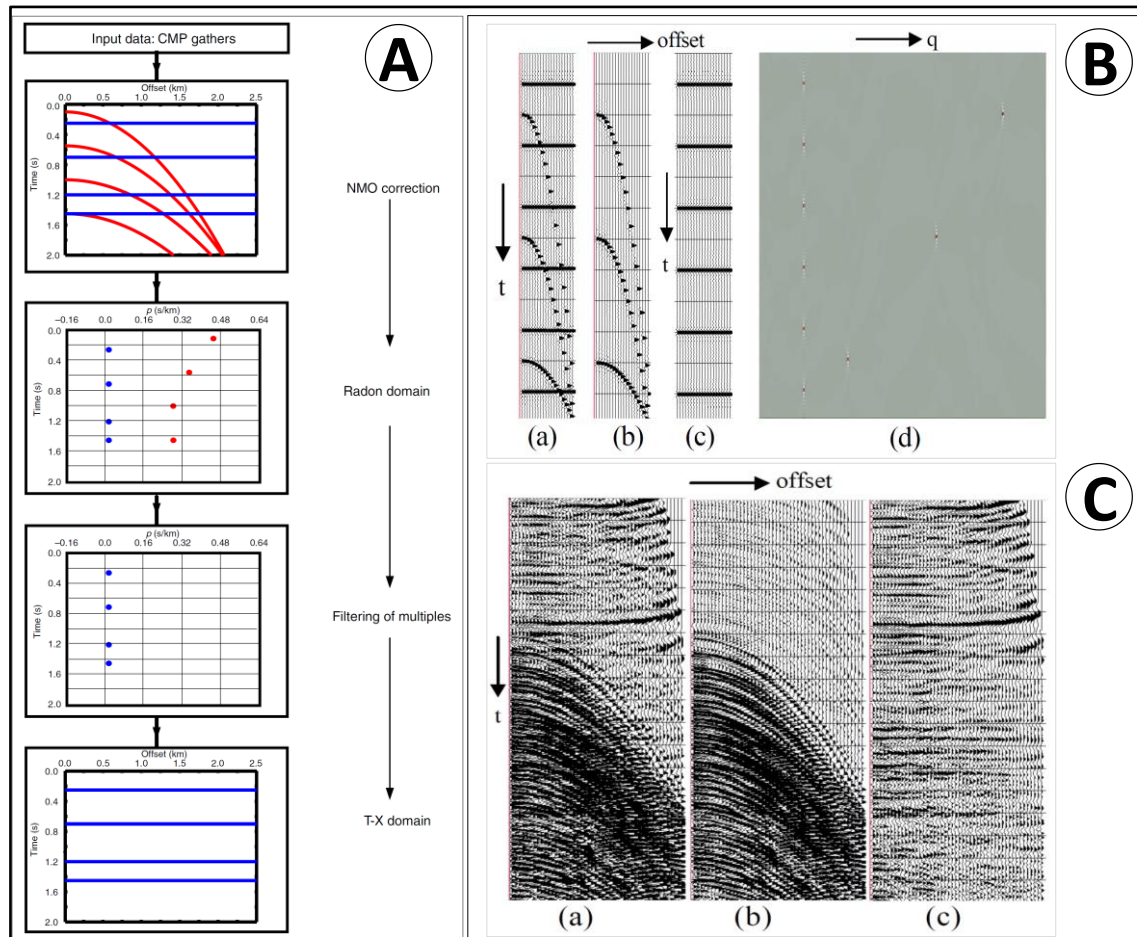


Fig. 4. (A) The main steps in the Radon demultiple. The primaries are blue lines (t-x) domain and blue circles (in the Radon domain). The multiples are red lines (t-x) domain and red circles in the Radon domain. (B) (a) Simulated NMO-corrected CMP. (b) Multiple models were reached using the DHR parabolic Radon transform. (c) Estimated primaries, (d) DHR parabolic Radon spectra. (C) (a) Input CMP gather, (b) a multiple model using DHR Radon transform; (c) estimated primaries (a)-(b) (modified from Herrmann *et al.*, 2000).

2D Seismic Data Acquisition and Processing

The seismic surveys are the initial phase in hydrocarbon exploration and development (E&D) (Gardi *et al.*, 2024). The new 2D land seismic dataset acquired in 2021 aims to characterize the structure, stratigraphy, and reservoir characterization of shallow targets and to image deep potential exploration targets. Table 1 summarizes acquisition parameters. In general, the multiple attenuation for land is not as easy to apply as for the marine data. The land data sets, however, reveal irregular geometry forms often combined with low S/N ratios and variable directivity patterns, resulting in erroneous multiple prediction operators. Additionally, the near-surface conditions (land) are quite different from those corresponding to the simple free surface of a marine environment. Thus, accurate pre-processing of the input data (before demultiple) is required. The processing flow is considered to make structural, stratigraphic interpretation, and AVO inversion more reliable and easier, as the original amplitude gain is preserved. The 2D seismic data processing has been carried out in the CGG's Geovation system with the following steps before demultiples as shown in Table 2. Figure 5 shows shot gathers before and after processing steps (steps 1 to 4).

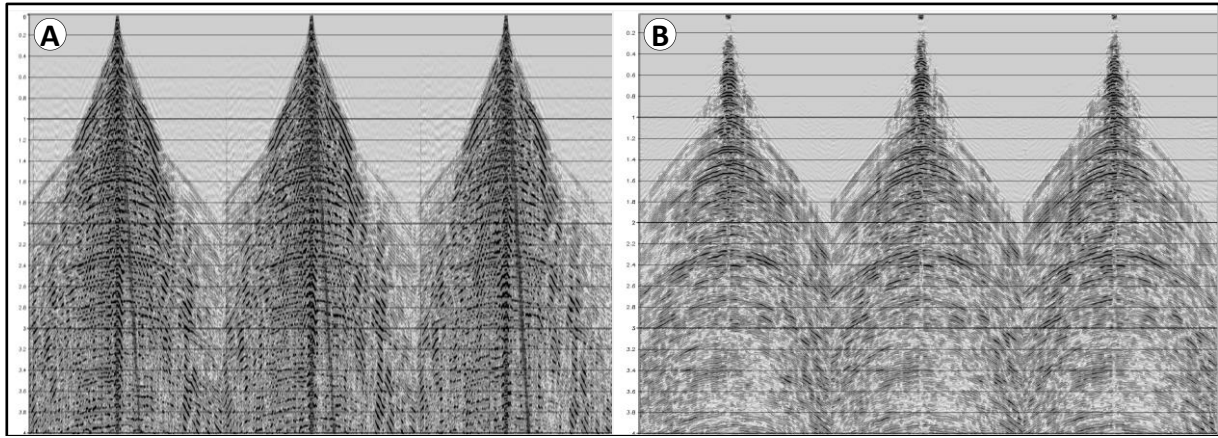


Fig. 5. Shot gathers (a) raw data; (b) after processing steps (1 to 4) according to Table 2. (X-axis time in ms).

Table 1: 2D seismic acquisition parameters.

Parameter		Parameter	
No. of Receiver lines/ active channels.	520/520	Sweep length	16 s
Receiver stations interval	25 m	No. of sweeps per location	4
Source stations interval	50 m	Receiver Type	Sensor SG-10 (12 R)
Nominal CDP fold	130	Number of strings per pattern	2 strings
Minimum offset	13.8 m	Geometry of the pattern	Linear
Maximum offset	6487 m	Pattern dimensions	96 m
No. of vibrators in the source pattern	4	Sampling interval	2 ms
Sweep type (linear up sweep)	7 Hz – 90 Hz,	Record length, Correlated	5 s

Table 2: Processing flow for the current 2D seismic data.

No	Processing Steps
1	Reformatting
2	Geometry Update
3	Spherical Divergence recovery
4	Noise Attenuation 1 st pass (Despike/Linear noise Attenuation / Ground-roll / Guide wave attenuation/F-K)
5	Refraction static computation
6	Surface consistent Amplitude correction (SCAC)
7	Noise Attenuation 2 nd pass
8	Surface consistent Deconvolution (Gap Decon).
9	Noise Attenuation 3 rd pass
10	Velocity (2km by 2km) (1 st pass)
11	Surface consistent Amplitude correction (2 nd pass)
12	Velocity (1km by 1km) (2 nd pass)
13	Surface consistent residual statics corrections 1 st pass.
14	2D Regularization
15	Noise Attenuation 4 th pass (offset class domain)
16	Velocity (1km by 1km) (3 rd pass)
17	Surface consistent residual statics corrections 2 nd pass.
18	Pre STM-Velocity Analysis 0.5 x 0.5km. (4 th pass)
19	Pre-Stack Kirchhoff time migration production
16	Velocity picking 0.5Km*0.5Km. (5 th pass)
20	High-resolution de-aliased multiple attenuations (post imaging).

In the current 2D seismic dataset, we try to attenuate multiple reflections using an anti-multiples module (τ -q domain) called RAMUR moduli in the CMP gathers (domain) to attenuate long-period multiples after applying all the pre-processing steps (before de-multiples) as aforementioned, including picking velocity (every 500 m). During processing steps, predictive deconvolution is applied to remove short-period multiples. The end outcome of the deconvolution procedure is a sharpened seismic wavelet with enhanced temporal resolution. Figure 6A and B show the stack and autocorrelation before and after gap deconvolution, and Figure 6C shows the amplitude spectrum.

The Input CDP gathers to Parabolic Radon (τ - q) transform and filter methods are based on velocity discrimination. The job is based on the assumption of hyperbolicity before NMO and parabolicity after NMO correction for attenuation of long-period multiples. The Parabolic transform sums along parabolic curves and creates constant curvature Stacks (CCS). The standard parabolic transform involves summing along a predefined range of parabolas. The parabola sampling rate is determined by a frequency-independent parameter, which has corrected NMO and tested mute for eliminating first break refractions and NMO stretch. Figure (7) shows the procedure of High-Resolution Radon demultiples attenuations.

The velocity-picking phase is carried out after the migration step. The picking is done on the 2-D pre-stack Kirchhoff time-migrated data with (500 m) intervals. The picking is done manually using semblance, gathers, and mini stacks using CGG's velocity analysis program (called Pacesetter). The use of dense interval distance picking is to define the optimum NMO correction of CDP gathers for stack and to allow for a more aggressive de-aliased High-Resolution Radon (HRD) de-multiples to be applied to attenuate multiples. Attention is paid to NMO-corrected gathers and stacks before and after analysis, ensuring that gathers are flattened and that stacks are improved. V_{rms} function and iso-velocity displays are also used for QC purposes. Figure 8 shows an example of the initial picking (every 1 km) and final PSTM velocity picking (every 0.5 km) for the de-multiple steps.

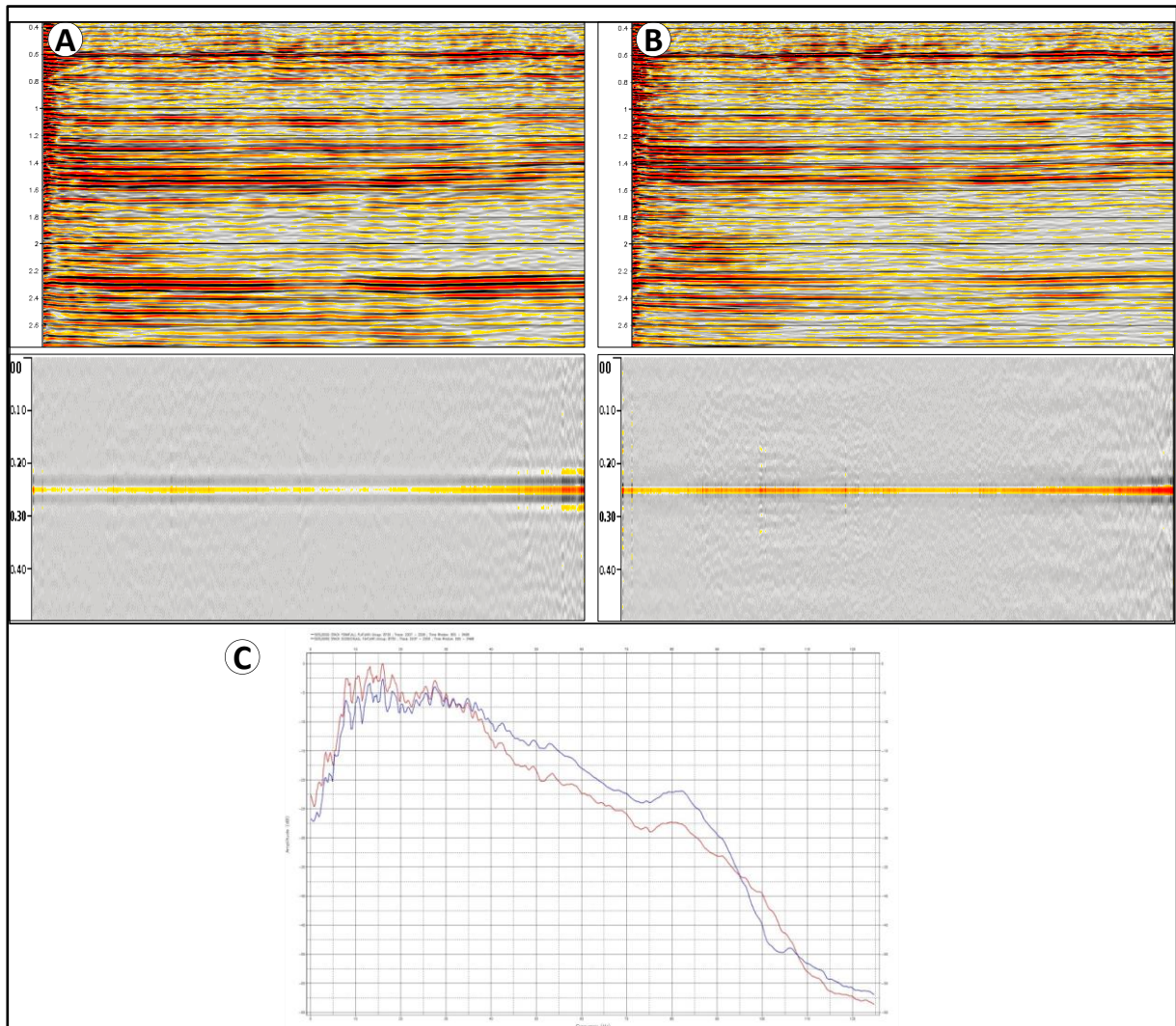


Fig. 6. (A) Stack and autocorrelation before gap deconvolution (X-axis time in ms); (B) after deconvolution (prediction gap (gap 24 ms); operator length of the filter (160 ms) for the current design window; (C) amplitude spectrum (X amplitude-Y frequency Hz) before (red) and after (blue) gap deconvolution. The spectrum calculation is made in a rectangular window: 250–2500 ms.

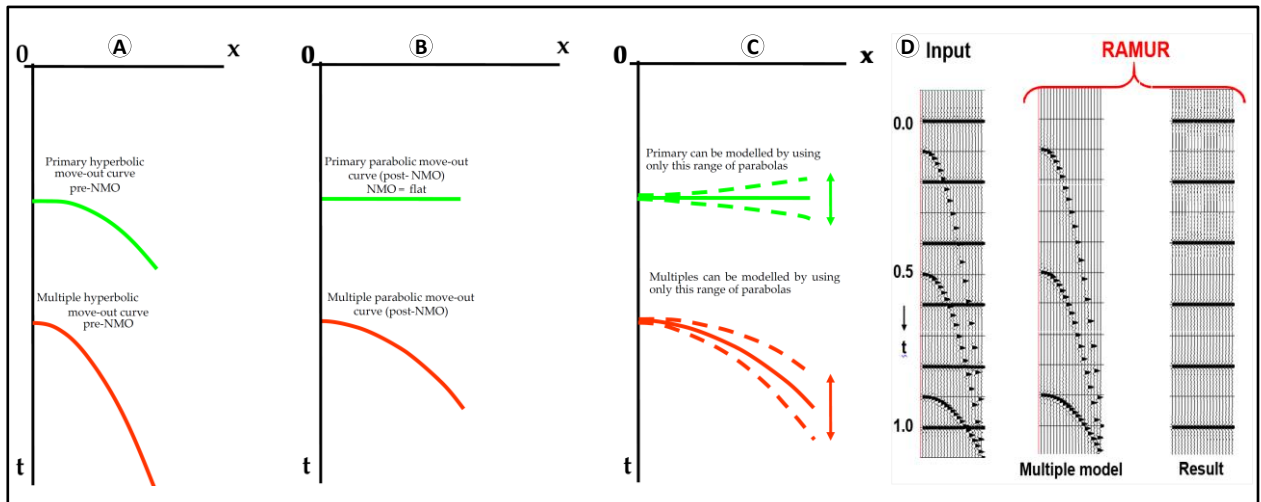


Fig. 7. Primary and Multiple Geometry (a) pre-NMO; (b) post-NMO; and (c) after NMO modelling along parabolas (d) HRD multiple attenuations (Compagnie Générale de Géophysique, CGG, 2011).

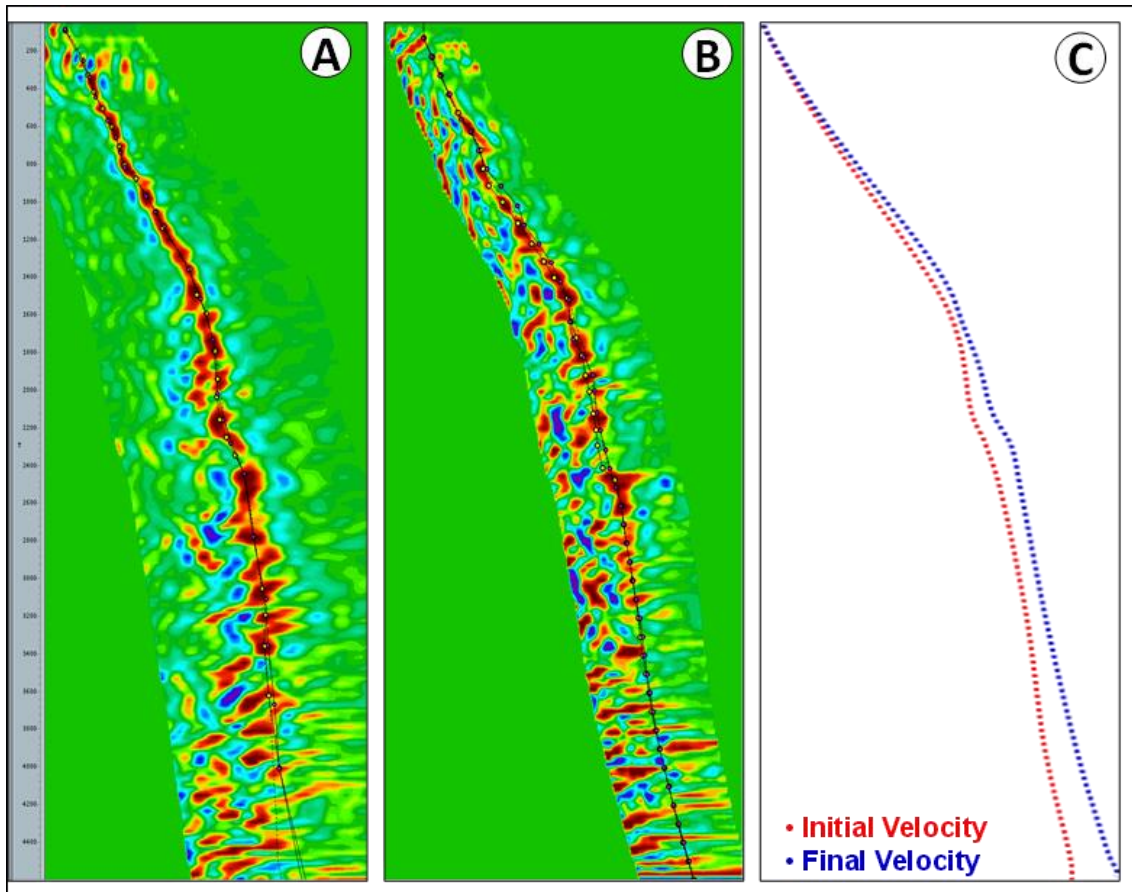


Fig. 8. Example of semblance velocity analysis panels for the same CMP (A) initial picking 1 km; (B) final PSTM velocity picking 0.5 km; (C) comparison stack velocity curves.

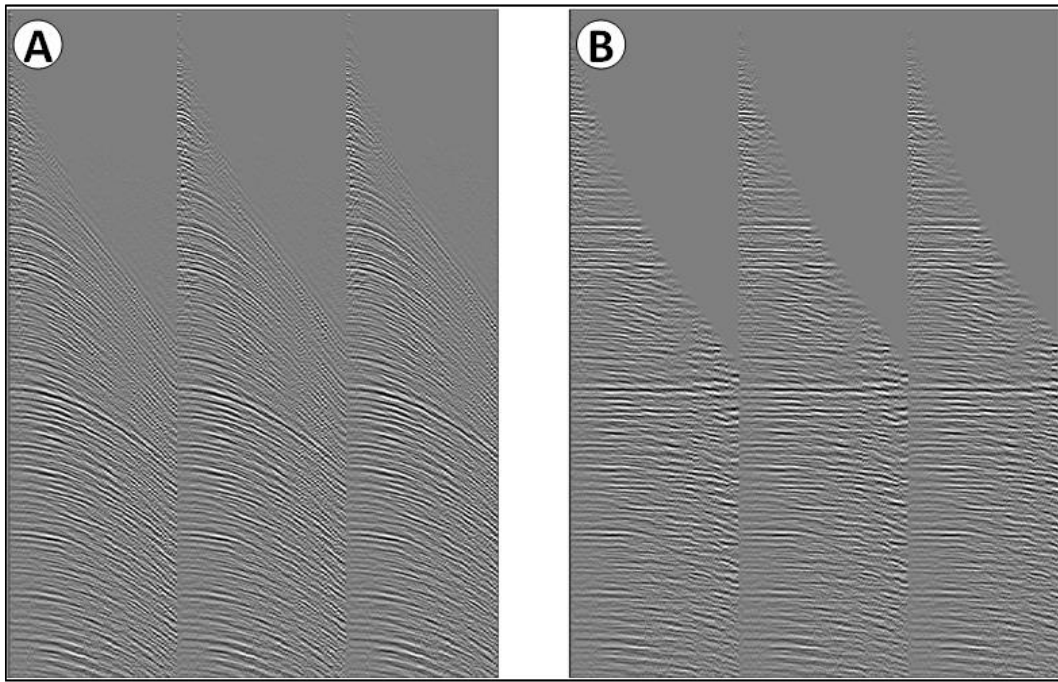


Fig. 9. CMP gathers (a) before and (b) after NMO Correction.

The multiple attenuation runs a model of primary and multiple reflection events. This computation is based on data decomposition into predefined parabolas and performed using a high-resolution, de-aliased least-squares (LS) method in the frequency-space (f - x) domain for each frequency of the pass-band defined by lower (DTMIN) and upper limit (DTMAX) for scanning parabolas, as well as frequency band definition minimum (FMIN), and maximum (FMAX) frequencies to process. The FMIN and FMAX ranges are selected by looking at the frequency spectrum of the data within the processing window. Reducing FMAX will reduce run times, but unfortunately, may also result in poorer multiple suppression. Hence, there is no need to process frequencies that will be filtered later in the processing steps. The calculation of models is performed only on the predefined frequency band. All other frequencies outside the processing band are left unchanged.

Seismic reflection events with a large curvature related to parabolas are considered to be multiples; in contrast, events smaller than this limit are considered to be primary reflection events. The zone limits between primaries and multiples are predefined based on tests. The difference between data and the sum of primary and multiple events is considered noise. The HRD multiple attenuation (RAMUR) subtracts the model of multiples or the model of multiples plus the noise from the input CMP gathers. The module has an algorithm that performs the computations. It is relatively efficient in terms of computation time, depending mainly on the number of traces (NC), spatial windows, and the number of p-traces (NP). Sometimes the algorithm gives approximate results, but with a high enough precision for usual cases. However, in the case of unacceptable results, the processor should make more tests. Figure 10 shows a schematic illustration and DHR key parameters for scanning of primary and multiple events. The procedure of carrying out HRD multiple attenuations (RAMUR module) is as the following steps:

1. RAMUR works on NMO-corrected CDP gathers to distinguish the residual curvatures of the multiples.
2. The previous step enables the processor to define essential RAMUR parameters (DTMIN, DTMAX, and DDT).
3. The values of DTMIN and DTMAX are given at the far-trace offset XRM.

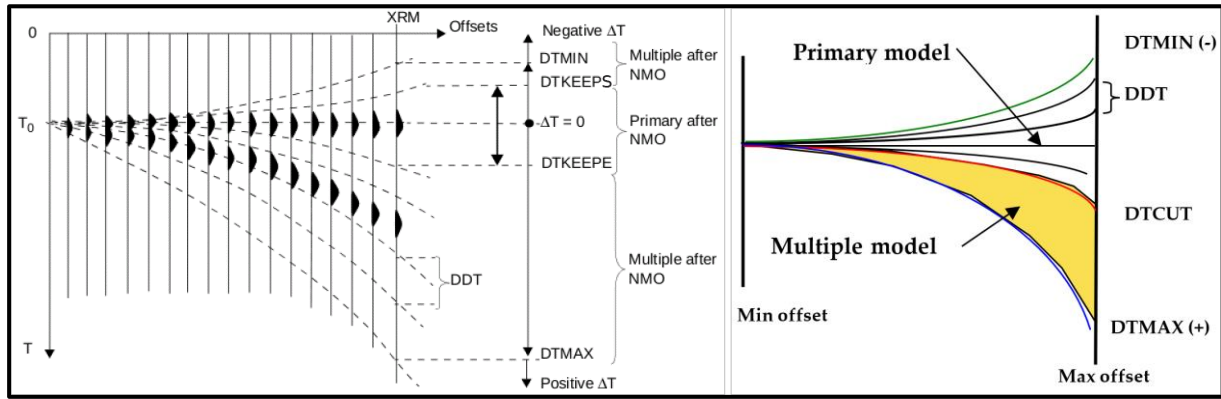


Fig. 10. Scanning of primaries and multiples according to parabolas (CGG, 2011).

Result and Discussion

We have carried out HR de-aliased multiple attenuation (RAMUR algorithm) tests on 2D seismic data with the combination of several key parameters, the tests have been made to determine the most suitable values for the increment between parabolas (DDT) parameter which controls the number of functions that are built, range of the lower and upper limit for scanning parabolas (DTMIN and DTMAX). To correctly model the primaries, the DTMIN parameter should always be negative. In general, the value of DTMIN is negative or null, and always smaller than DTMAX. Also, test taper application, e.g., the taper length centered on the separating threshold curves and applied to parabolas. The zone limiting the domain between primaries and multiples model (DTCUT) is a predefined parameter cut-off at far offset (XRM).

The HR radon de-aliased multiple attenuation testing consists of the following DTCUT trials: 100, 200, 300, 350, 400, 500, and 1000 ms at (XRM=6525 m). We have tested DTCUT at far offset from the start time (TI) 1000, 1500, 2000, and 3000 ms with a taper of 200 ms with DTMIN (-100, -130, -150, -170, 200) ms and DTMAX (2000, 3000, 4000, and 4500 ms). In addition, various window lengths (XCX) are tested for filter design (100, 200, 300, 400, and 500); In general, the smaller window size is expected when the subtraction touches the primary event. Lastly, we choose a filter window of 500 ms \times 21 traces based on a visual judgment of a balance between primary retention and multiple attenuations in the CMP domain. DTMIN (-170 ms) and DTMAX (5000 ms) are recommended for optimum parabolic Radon transformation and results. The initial time is applied at 1000 ms to avoid attenuating primary energy in the shallow beds. Table 3 summarizes some test parameters used for the HR de-aliased multiple attenuation (RAMUR) algorithm.

Table 3: Some test parameters applied for HR de-aliased multiple attenuation (RAMUR algorithm).

TEST	DTCUT (ms)	Initial Time (IT) (ms)	FMAX (Hz)
01	100	1000	80
02	200	1000	80
03	300	1000	80
04	350	1000	80
05	500	1000	80
06	1000	1000	80
07	300	1000	80
08	300	1500	80
09	300	2000	80
10	300	3000	80
11	300	1000	70
12	300	1000	100
13	300	1000	125

Figure (11) shows CMP gathers before, after, and difference demultiples with used DDT 12 ms; initial time 1000 ms, and DTMAX tests (2000, 3000, and 4000) with DTMIN (-300).

Figure (12) shows CMP gathers with DDT 12; initial time 1000 ms with DTCUT (200, 350). Table (4) summarizes the recommended choice the parameter values after accomplishing a large number of tests.

Table 4: Recommended parameters applied for HR de-aliased multiple attenuation.

Parameters	Value
Processing window (XCX)	500 ms
FMIN-FMAX	10-80 Hz
Far trace offset (XRM)	6525 m
The final time of the processing (TF)	5000 ms
No. of traces (NC)	200
Length of the temporal elementary (NCT)	500
Separation threshold (DTCUTS)	170 ms
Second separation threshold (DTCUTE)	4000 ms
The lower limit for scanning parabolas (DTMIN)	-170 ms
Upper limit for scanning parabolas (DTMAX)	5000 ms
The increment between parabolas (DDT)	12 ms
DTKEEPS	-250 ms
DTKEEPE	350 ms

We attempt to suppress both long and short-period multiples using the moveout discrimination method. We execute multiple attenuations in the Radon domain. NMO correction is performed using the picked RMS velocity to flatten primary events, and the CMP gathers are transformed into the Radon domain using the least-squares-parabolic Radon transform. It is found during tests that the range of the upper limit for scanning parabolas, DTMAX, has a main effect on the resulting primaries, whereas the lower limit for scanning parabolas, DTMIN, has only a marginal effect. Among various parameter combinations, we see sections overly cleaned and dominated by low frequency at small DTMIN and large DTMAX. The multiple reflections and noise can be removed when decreasing the separation threshold (DTCUT) compared with other results. The presence of multiple under the at times 1000 ms is a long-period multiple, which has a large wave arrival time. After multiple event reductions using the RAMUR algorithm, it is quite effective in reducing the presence of long-period multiple events. Figure 13 shows colored CMP gathers before and after DHR multiple attenuations by applying recommended parameters. Figure (14) shows gray-scale CMP gathers, before, after, and with multiple energies removed. Figure (15) magnifies the stack section before and after HR Radon demultiple with the difference (energy removed). Figure 16 magnifies the stack wiggle section of the input and subtraction result obtained by RAMUR. In addition, the signal will be enhanced because of the removal of multiple and random noises, as shown by the spectrum of Figure 17.

The result proves that demultiple using the high-resolution Radon demultiple method in land seismic areas can eliminate the multiples, especially long-period multiples. The Radon transformation method is very effective and more efficient, with more accurate velocity picking in separating primary and multiple signals. In general, it can be stated that demultiple via the parabolic Radon domain can deliver good results. However, it will work at its best in areas with reasonably simple geology without strong lateral velocity and structural variations, as this will ensure that residual move-outs of the multiples can be approximated with parabolas. The high-resolution parabolic Radon transform is also better capable of handling spatial aliasing effects.

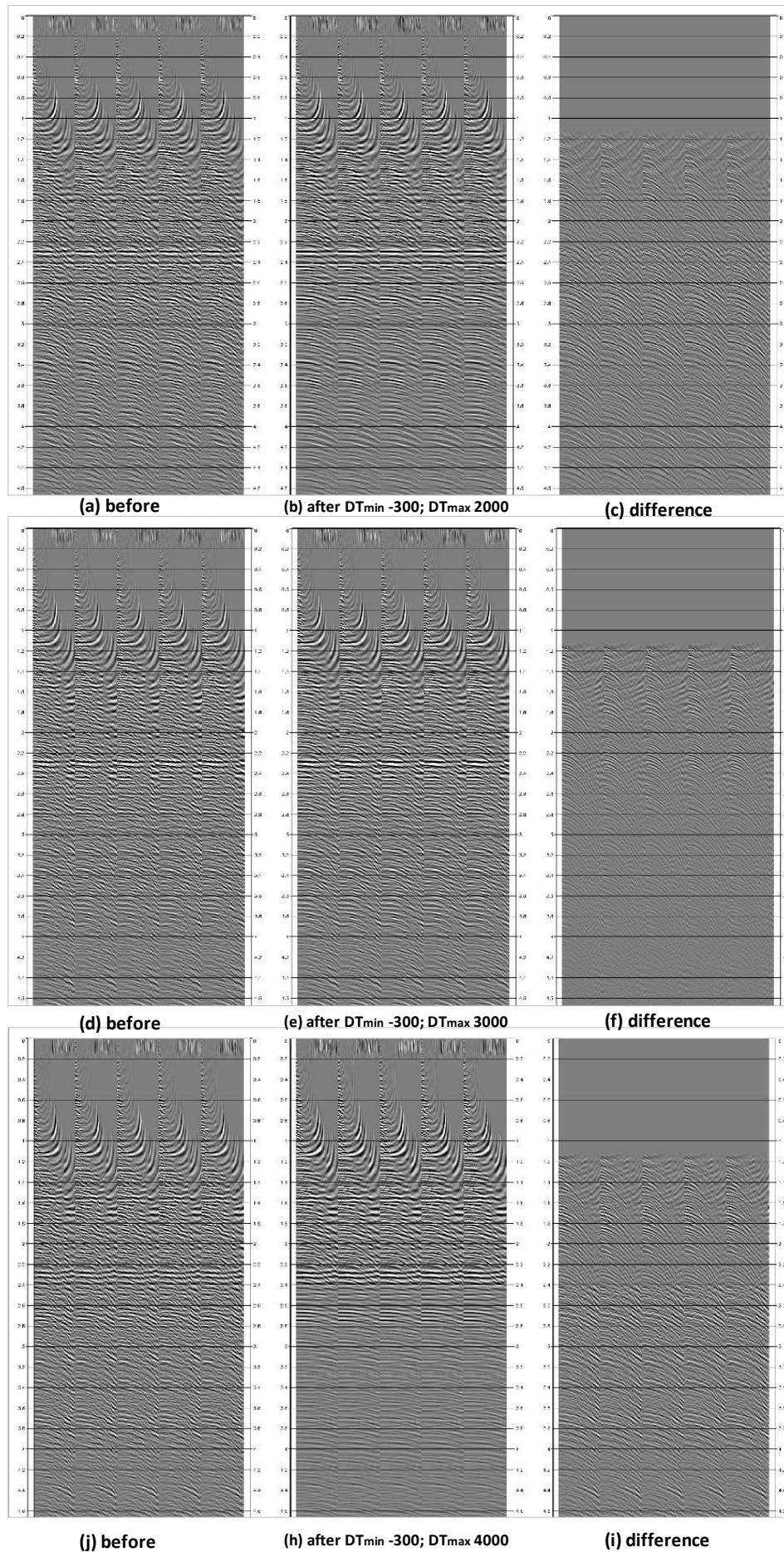


Fig.11. CMP gathers (a, d, j) before, (b, e, h) after, and (c, f, i) difference. DHR demultiples with tested parameters (DT_{min} and DT_{max}) and uses DDT 12; initial time 1000 ms. (X-axis time from zero to 4.6 sec)

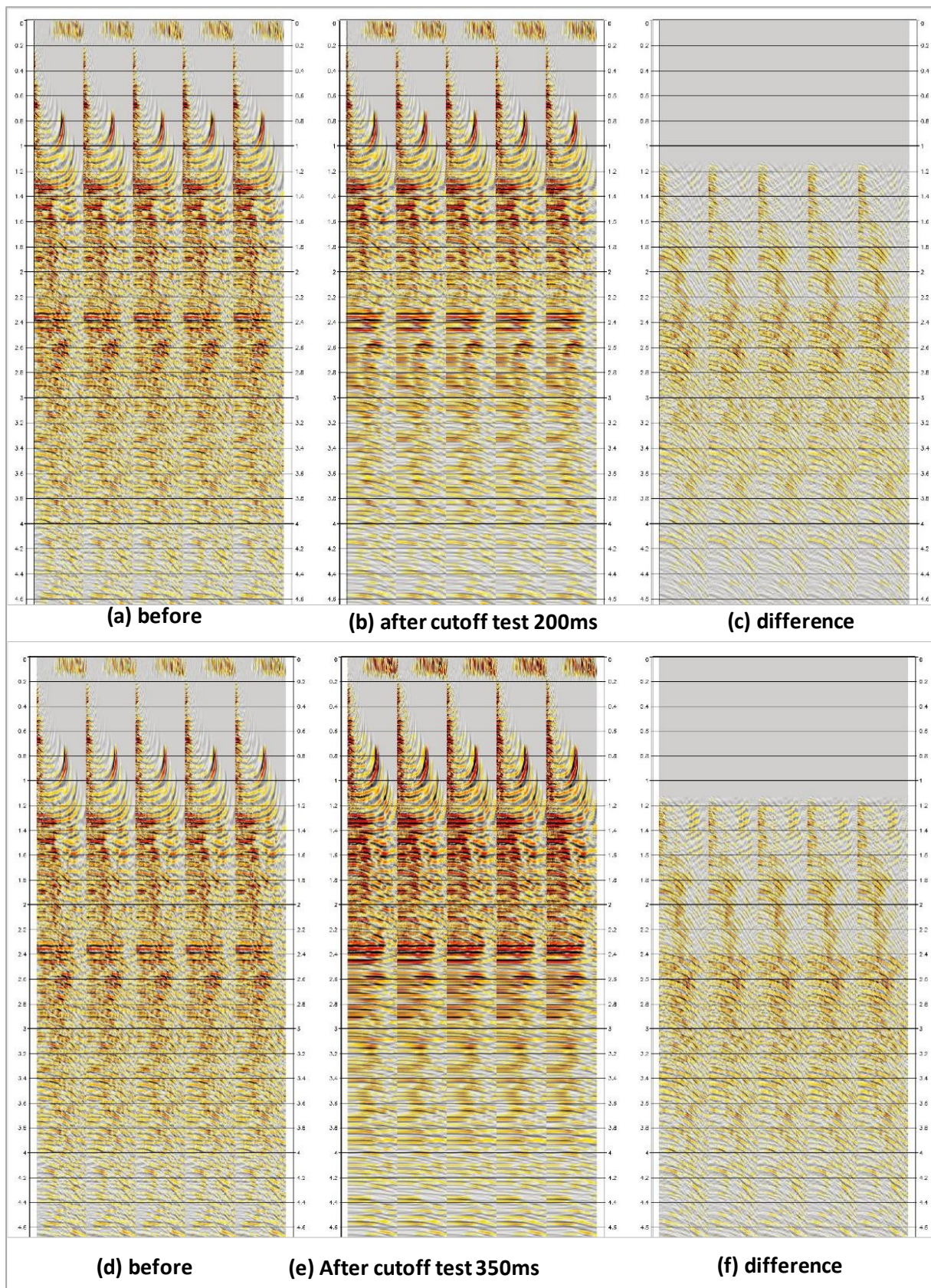


Fig. 12. CMP gathers (a, d) before; (b, e) after; and (c, f) difference DHR demultiples with used DDT 12; initial time 1000 ms (X-axis time from zero to 4.5 sec)

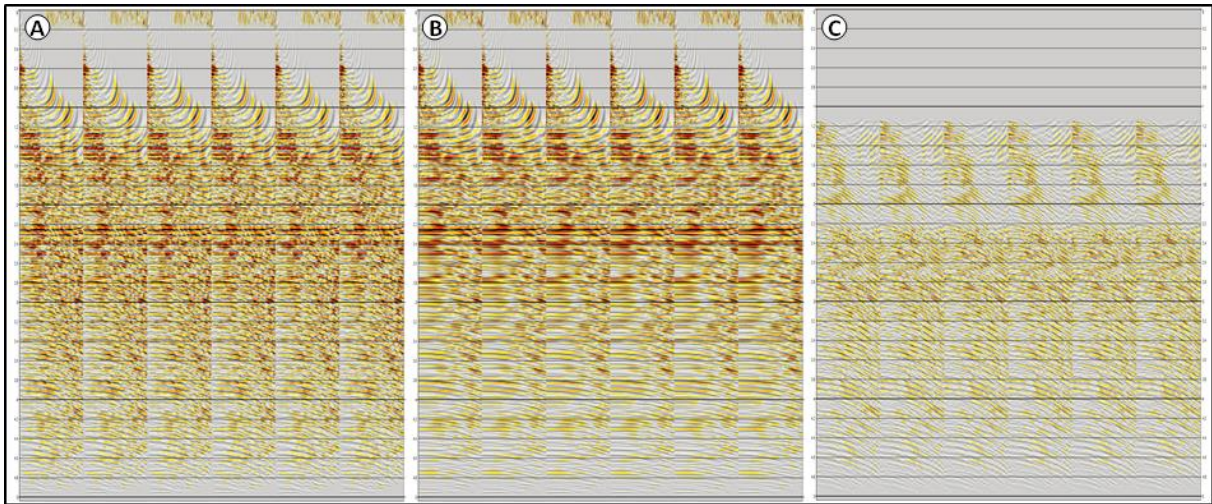


Fig. 13. CMP gathers (a) before; (b) after; and (c) difference DHR multiple attenuation.

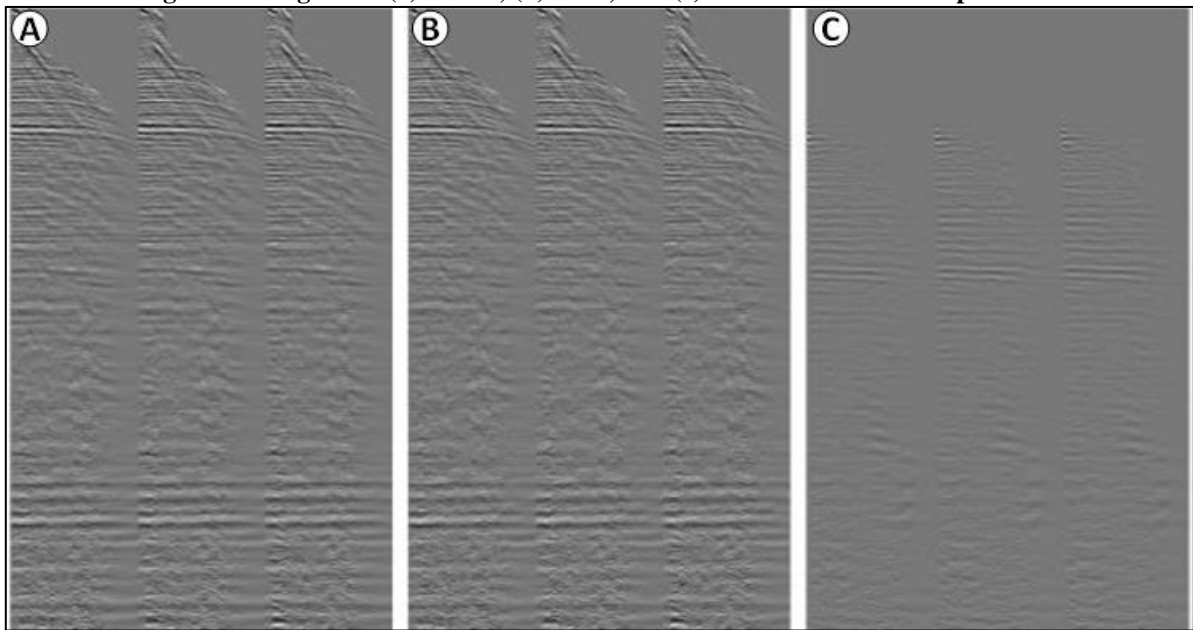


Fig. 14. Gray-scale image CMP gathers, before (a), after (b) RAMUR, and the multiple energy removed by RAMUR (c). (X-axis time from zero to 4 sec)

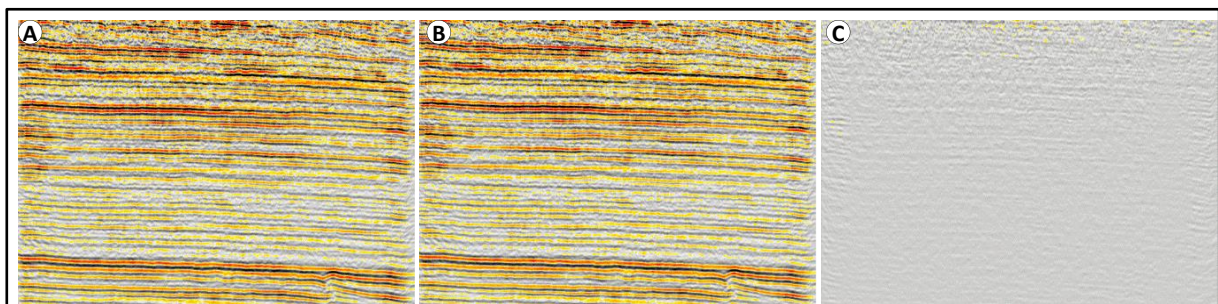


Fig. 15. (a) Magnified stack section from (1.2 to 2.3 sec) (a) before; (b) after HR Radon de-multiple and (c) Stack difference.

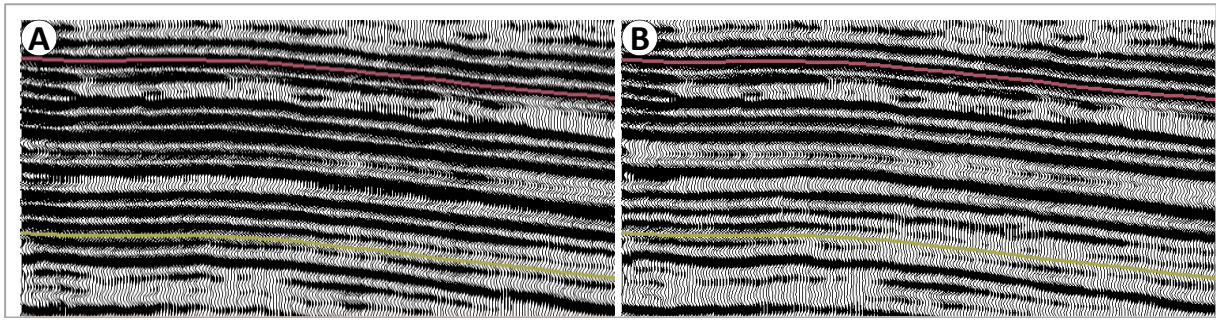


Fig. 16. Magnified stack wiggle section from (0.8 to 1.5 sec) of the (a) input and (b) subtraction result obtained by RAMUR.

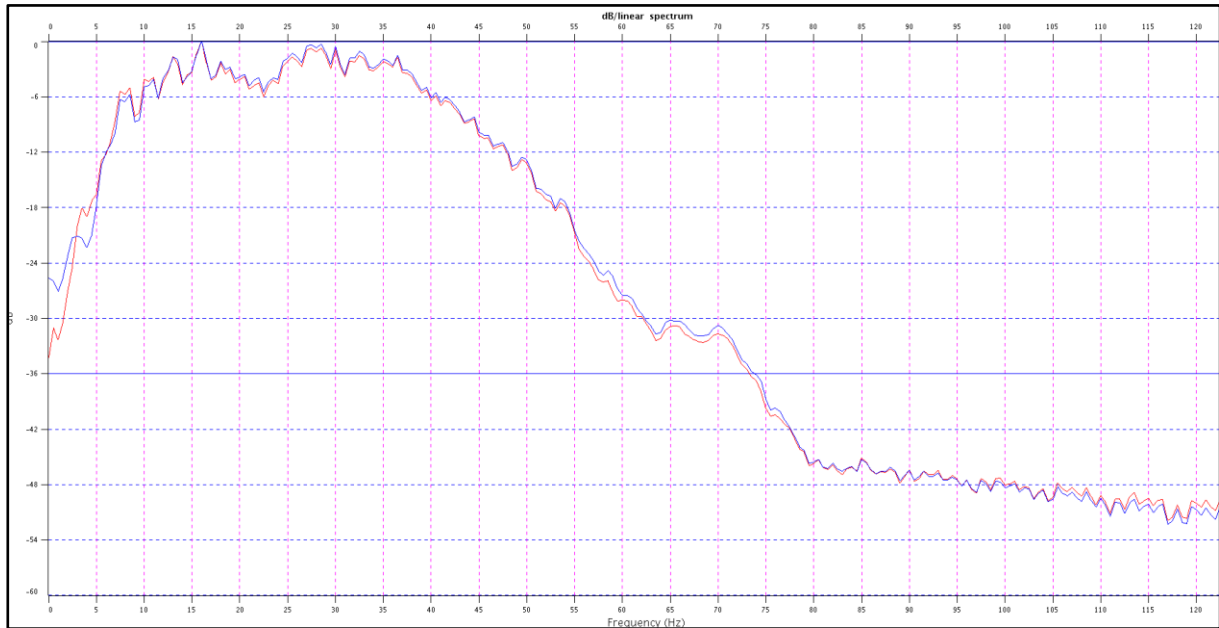


Fig. 17. Amplitude- frequency spectrum before and after demultiples (X-amplitude from zero to 60dB; Y-frequency from zero to 120 Hz before (red) and after (blue). The spectrum is calculated in a rectangular window: 500–2500 ms.

Conclusion

The application of the HR parabolic radon multiple attenuation technique depends on the multiple events' properties in seismic data, such as frequency and NMO velocity. Because the VSP data are not available in practice, a good processing flow must be applied, as well as CMP normal move-out (NMO correction) must be accurate before multiple attenuation to handle and speared primaries and multiples.

We contribute a comprehensive introduction and overview of the demultiple technique with Parabolic Radon and HR Parabolic Radon.

1. De-aliased High-Resolution Radon subtraction (RAMUR algorithm) is tested on the 2D Seismic data acquired in Iraq.
2. Parabolic Radon transform is an effective method in attenuating multiple reflections based on velocity analysis. Applying this method makes it possible to attenuate a large range of multiple reflections with different trajectories.
3. The de-multiple procedure is a combination of the prediction method based on wavefront characteristics of multiple generating primary reflections and the Radon transform-based method for multiple subtractions.
4. After a proper selection flow for key parameters (DTCUT, DDT, DMAX, and FMAX) is used to handle multiple events. Radon Transform successfully attenuates multiples with High-Resolution Radon De-multiple (RAMUR), indicating that the HR can

effectively and successfully separate the multiples from the primaries in seismic data, and produce seismic data without multiples.

5. The HR radon demultiple is efficient in removing a significant number of coherent events. The seismic CMP gathers tend to demonstrate this process as beneficial in pre-stack data cleaning. Stack display and differences show that flat events are attenuated between 1.2 and 3.0 seconds.
6. It is not easy to identify if the changes in this related amplitude are related to multiple contaminating primaries or real primary energy. However, the gathered quality control (QC) seems to confirm that primary energy is preserved.
7. As the demand for computing resources is not extremely high, we recommend RAMUR as a basic processing flow for 2D seismic data without any knowledge about the subsurface, especially in the western and southwestern parts of Iraq.

References

- Al Mukhtar, K.S. and Alsayadi, A.A., 2015. Processing and Interpretation of 3D Seismic Data of an Oil Field in Central Iraq Using AVO Techniques. *Iraqi Journal of Science*, 56(2C), pp. 1728–1738. <https://ijs.uobaghdad.edu.iq/index.php/eijs/article/view/10024>
- Al-Ameri, T., Jafar, M. and Pitman, J., 2012. Hydrocarbon Generation Modeling of the Basrah Oil Fields, Southern Iraq. *GEO2012*, Bahrain. <https://doi.org/10.3997/2214-4609-pdb.287.1176781>
- Al-Heety, A.J.R. and Thabit, H.A., 2022. Random and Coherent Noise Attenuation for 2D Land Seismic Reflection Line Acquired in Iraq. *NRIAG Journal of Astronomy and Geophysics*, 11(1), pp. 337–354. <https://doi.org/10.1080/20909977.2022.2118982>
- Al-Sakini, J.A., 1995. Neo-tectonic Events as an Indicator to Determine the Oil Structures in the Mesopotamian Fields, in 3rd Geological Conference, pp. 130–142.
- Al-Shuhail, A. and Al-Dossary, S., 2020. Attenuation of Incoherent Seismic Noise, 1st Edition, XIV, 182 P. Springer Cham, Springer Nature Switzerland AG. <https://doi.org/10.1007/978-3-030-32948-8>
- Alvarez, G., 1995. A Comparison of Moveout-Based Approaches to the Suppression of Ground-Roll and Multiples, PhD Thesis, Colorado School of Mines.
- Alvarez, G., 2001. Multiple Suppression With Land Data: A Case Study. *Stanford Exploration Project*, Report, pp. 1–13.
- Cary, P.W., 1998. The Simplest Discrete Radon Transform. *SEG Technical Program Expanded Abstracts 1998*, pp. 1999–2002. <https://doi.org/10.1190/1.1820335>
- CGG, 2011, *Geovation User's Manual*. CGG-Varitas Company. France.
- Dix, C.H., 1948. The Existence of Multiple Reflections. *Geophysics*, 13(1), pp. 49–50. <https://doi.org/10.1190/1.1437370>
- Dragoset, W.H. and Jeričević, Ž., 1998. Some Remarks on Surface Multiple Attenuations. *Geophysics*, 63(2), pp. 772–789. <https://doi.org/10.1190/1.1444377>
- Foster, D.J. and Mosher, C.C., 1992. Suppression of Multiple Reflections Using the Radon Transform. *Geophysics*, 57(3), pp. 386–395. <https://doi.org/10.1190/1.1443253>
- Fouad, S. F., 2012. *Tectonic Map of Iraq*, Scale 1: 1000 000, 3rd Ed. GEOSURV, Baghdad, Iraq.
- Gardi, K.I., Aziz B.Q. and Baban E.N., 2024. Seismic, Petrophysics, and Attribute Analysis to Evaluate the Tertiary Reservoir in the High-Folded Zone, Kurdistan Region-Iraq. *Iraqi*

- National Journal of Earth Science (INJES).
<https://doi.org/10.33899/earth.2023.142239.1121>
- Geldart, L.P. and Sheriff, R.E., 2004. Problems in Exploration Seismology and Their Solutions. Society of Exploration Geophysicists.
- Gutenberg, B. and Fu, C.Y., 1948. Remarks on Multiple Reflections. *Geophysics*, 13(1), pp. 45–48. <https://doi.org/10.1190/1.1437368>
- Hampson, D., 1986. Inverse Velocity Stacking for Multiple Elimination. In SEG Technical Program Expanded Abstracts 1986, pp. 422–424. SEG.
<https://doi.org/10.1190/1.1893060>
- Hansen, R.F. and Johnson, C.H., 1948. Multiple Reflections of Seismic Energy. *Geophysics*, 13(1), pp. 58–85. <https://doi.org/10.1190/1.1437377>
- Hargreaves, N. and Cooper, N., 2001. High-Resolution Radon Demultiple. 2001 SEG Annual Meeting. <https://doi.org/10.1190/1.1816341>
- Herrmann, P., Mojesky, T., Magesan, M. and Hugonnet, P., 2000. De-Aliased, High-Resolution Radon Transforms. SEG Technical Program Expanded Abstracts 2000, pp. 1953–1956. <https://doi.org/10.1190/1.1815818>
- Hugonnet, P. and Canadas, G., 1997. Regridding of Irregular Data Using 3D Radon Decompositions. SEG Technical Program Expanded Abstracts 1997, pp. 1111–1114. <https://doi.org/10.1190/1.1885585>
- Hugonnet, P., L. Boelle, J., Mihoub, M. and Herrmann, P., 2009. 3D High-Resolution Parabolic Radon Filtering. 71st EAGE Conference and Exhibition Incorporating SPE EUROPEC 2009. 71st EAGE Conference and Exhibition incorporating SPE EUROPEC 2009, Amsterdam, Netherlands. <https://doi.org/10.3997/2214-4609.201400428>
- Ibrahim, A., Sacchi, M.D. and Terenghi, P., 2015. Wavefield Reconstruction Using a Stolt-Based Asymptote and Apex Shifted Hyperbolic Radon Transform. SEG Technical Program Expanded Abstracts 2015, pp. 3836–3841. <https://doi.org/10.1190/segam2015-5873567.1>
- Iverson, A., Perez, M. and Holt, R., 2014. The Impact of Interbed Multiples on the Inversion and Interpretation of Pre-Stack Data. *CSEG Recorder*, 39(1), pp. 36–41.
- Jassim, S.Z. and Goff, J.C., 2006. *Geology of Iraq*. 1st Edition, published by Dolin, Prague and Moravian Museum, Brno, printed in the Czech Republic.
- Kakhkhorov, U., 2019. Seismic Imaging with Primaries and Multiples, MSc Thesis, University of Stavanger, Norway.
- Lacombe, C., Hoeber, H., Souvannavong, V., Blaszcak, M. and Pradhan, P., 2019. Demultiple Techniques with Improved AVO Compliance. 81st EAGE Conference and Exhibition 2019, 2019(1), pp. 1–5.
- Li, C. and Yue, W., 2017. High-Resolution Radon Transforms for Improved Dipole Acoustic Imaging: High-Resolution Radon Transforms. *Geophysical Prospecting*, 65(2), pp. 467–484. <https://doi.org/10.1111/1365-2478.12434>
- Li, Z. and Gao, H., 2020. Feature Extraction Based on the Convolutional Neural Network for Adaptive Multiple Subtraction. *Marine Geophysical Research*, 41, pp. 1–20. DOI: [10.1007/s11001-020-09409-7](https://doi.org/10.1007/s11001-020-09409-7)
- Li, Z. and Lu, W., 2014. Demultiple Strategy Combining Radon Filtering and Radon Domain Adaptive Multiple Subtraction. *Journal of Applied Geophysics*, 103, pp. 1–11. <https://doi.org/10.1016/j.jappgeo.2014.01.004>

- Li, Z., Sun, N., Gao, H., Qin, N. and Li, Z., 2021. Adaptive Subtraction Based on U-Net for Removing Seismic Multiples. *IEEE Transactions on Geoscience and Remote Sensing*, 59(11), pp. 9796–9812.
- Mahdad, A., Doulgeris, P., and Blacquiere, G., 2011. Separation of Blended Data by Iterative Estimation and Subtraction of Blending Interference Noise. *GEOPHYSICS*, 76(3), Q9–Q17. <https://doi.org/10.1190/1.3556597>
- Marlow, L.M., Kendall, C.G.S.C. and Yose, L.A., 2014. *Petroleum Systems of the Tethyan Region*. American Association of Petroleum Geologists, Tulsa.
- Moore, I. and Dragoset, B., 2008. General Surface Multiple Prediction: A Flexible 3D SRME Algorithm. *First Break*, 26(9).
- Nowak, E.J. and Imhof, M.G., 2006. Amplitude Preservation of Radon-Based Multiple-Removal Filters. *GEOPHYSICS*, 71(5), V123–V126. DOI: [10.1190/1.2243711](https://doi.org/10.1190/1.2243711)
- Owen, R.M.S. and Nasr, S., 1958. Stratigraphy of the Kuwait-Basra Area. In Weeks, L.G., Ed., *Habitat of Oil*. AAPG, Memoir 1, pp. 1252–1278.
- Ramos, A.C., Oliveira, A.S. and Tygel, M., 1999. The Impact of True Amplitude DMO on Amplitude Versus Offset. In *SEG Technical Program Expanded Abstracts 1999*, pp. 832–835, Society of Exploration Geophysicists.
- Riley, D.C. and Claerbout, J.F., 1976. 2-D Multiple Reflections. *Geophysics*, 41(4), pp. 592–620.
- Sacchi, M.D. and Porsani, M., 1999. Fast High Resolution Parabolic Radon Transform. *SEG Technical Program Expanded Abstracts 1999*, pp. 1477–1480. DOI: [10.1190/1.1820798](https://doi.org/10.1190/1.1820798)
- Sacchi, M.D. and Ulrych, T.J., 1995. High-Resolution Velocity Gathers and Offset Space Reconstruction. *Geophysics*, 60(4), pp. 1169–1177.
- Schonewille, M.A. and Aaron, P.A., 2007. Applications of Time-Domain High-Resolution Radon Demultiple. In *SEG Technical Program Expanded Abstracts 2007*, pp. 2565-2569, Society of Exploration Geophysicists.
- Sengbush, R.L., 1983. Multiple Reflections. In *Seismic Exploration Methods*, pp. 103-123, Springer.
- Sheriff, R.E. and Geldart, L.P., 1995. *Exploration Seismology*. Cambridge University Press.
- Song, H., Mao, W., Tang, H., Xu, Q. and Ouyang, W., 2022. Multiple Attenuation Based on Connected-Component Analysis and High-Resolution Parabolic Radon Transform. *Journal of Applied Geophysics*, 199, 104580. DOI: [10.1016/j.jappgeo.2022.104580](https://doi.org/10.1016/j.jappgeo.2022.104580)
- Taner, M.T., 1980. Long Period Sea-Floor Multiples and Their Suppression. *Geophysical Prospecting*, 28(1), pp. 30–48.
- Tao, L., Ren, H., Ye, Y. and Jiang, J., 2022. Seismic Surface-Related Multiples Suppression Based on SAGAN. *IEEE Geoscience and Remote Sensing Letters*, 19, pp. 1–5.
- Trad, D., 2003. Interpolation and Multiple Attenuation With Migration Operators. *Geophysics*, 68(6), pp. 2043–2054.
- Treitel, S., 1969. Predictive Deconvolution-Theory and Practice. *Geophysics*, 34(2), pp. 155–169.
- Trinks, I., 2000. Removing Multiples from the Wide-Angle Wavefield. *Lithos Science Report*, 2, pp. 113–116.
- Verschuur, D.J., Berkhout, A.J. and Wapenaar, C.P.A., 1992. Adaptive Surface-Related Multiple Elimination. *Geophysics*, 57(9), pp. 1166–1177.

- Wang, K., Hu, T., Wang, S. and Wei, J., 2022. Seismic Multiple Suppression Based on a Deep Neural Network Method for Marine Data. *Geophysics*, 87(4), pp. V341–V365.
- Wang, Y., 2004. Multiple Prediction Through Inversion: A Fully Data-Driven Concept for Surface-Related Multiple Attenuation. *Geophysics*, 69(2), pp. 547–553.
- Wang, Z.S., Su, W.Q., Li, Y.X., Li, Z.S. and Hu, J., 2023. Seismic Forward Modeling of Acoustic Surface-Related Order-Separated Multiples. *Marine Geophysical Research*, 44(1), 3.
- Waterman, J.C., 1948. Multiple-Reflection Evidence, San Joaquin Valley, California, *Geophysics*, 13(1), pp. 41–44.
- Weglein, A.B., 1995. Multiple Attenuation: Recent Advances and the Road Ahead. In *SEG Technical Program Expanded Abstracts 1995*, pp. 1492–1495, Society of Exploration Geophysicists.
- Weglein, A. B., 1999. Multiple Attenuation: An Overview of Recent Advances and the Road Ahead (1999), *The Leading Edge*, 18(1), pp. 40–44.
- Weglein, A.B., Gasparotto, F.A., Carvalho, P.M. and Stolt, R.H., 1997. An Inverse-Scattering Series Method for Attenuating Multiples in Seismic Reflection Data. *Geophysics*, 62(6), pp. 1975–1989.
- Xiao, C., Bancroft, J.C., Brown, R.J. and Cao, Z., 2003. Multiple Suppression: A Literature Review. *CREWES Annual Report*, 15 P.
- Xue, Y., Yang, J., Ma, J. and Chen, Y., 2016. Amplitude-Preserving Nonlinear Adaptive Multiple Attenuation Using the High-Order Sparse Radon Transform. *Journal of Geophysics and Engineering*, 13(3), pp. 207–219.<https://doi.org/10.1088/1742-2132/13/3/207>
- Yilmaz, Ö., 2001. *Seismic Data Analysis: Processing, Inversion, and Interpretation of Seismic Data*, Society of Exploration Geophysicists.
- Yilmaz, O. and Doherty, S.M., 1987. *Seismic Data Processing: Investigations in Geophysics*, Society of Exploration Geophysicists, 2, 526 P.
- Yousif, F.H. Aziz B.Q., and Baban E.N., 2022. Oil Reservoir Detection Using Volume Attributes in Chia Surkh Area, Kurdistan Region, Iraq, *Science Journal of University of Zakho* 10.4 (2022), pp. 163-168.